Structural, Dielectric and Electrical Properties of Fe Doped $La_{0.7}Ba_{0.3}MnO_3$ Solid Solutions for Cathode Materials

Surinder Paul, Manokamna, Shubhpreet Kaur, P.S. Malhi, Anupinder Singh, Arvind Kumar

Abstract: The solid solutions of $(La_{0.7}Ba_{0.3})(Fe_xMn_{1-x})O_3$ where x = 0.1 - 0.5 ceramics were synthesized by conventional solid-state method. The structural analysis was done by X-Ray diffraction technique and the results have revealed that all the samples were crystallized into a single phase. The surface morphology was done by Scanning Electron Microscopy and the micrographs clearly indicate decreased grain size with the increasing Fe - concentration. The density of the prepared samples was done using Archimedes principle and the density values were found to be in decreasing order, which is well in agreement with the microstructure relationship. The dielectric and impedance properties have been studied at different ranges of frequency and temperature. The electrical conductivity values were found to be greater than 100 Scm^{-1}, which suggests it to suitable cathode material of SOFCs.
Index Terms: Solid Oxide Fuel Cell, SOFC, Cathode Material, Magnites

I. INTRODUCTION

Solid oxide fuel cells (SOFCs) are one of the attractive alternative energy sources due to its relatively inexpensiveness, low sensitivity to impurities, and high efficiency [1-4]. SOFCs have developed a great interest due to its versatile applications [5-7]. The SOFC has three major components (a) Anode, (b) Cathode and (c) Electrolyte. There are some requirements to be fulfilled by the synthesized cathode material, such as, cathode material to operate at temperatures greater than 600°C (operating temperature range of the intermediate SOFCs) and electrical conductivity to be more than 100 Scm^{-1} in the operating temperature range [1]. Therefore, the materials being synthesized are to fulfill the above requirements to be called as suitable cathode material. In addition, mechanical and chemical compatibility issues are also to taken into consideration.

There are some perovskite materials such as $LaMnO_3$, $LaCoO_3$, and $LaFeO_3$ and their solid solutions with suitable ion substitutions, suggested and used to be cathode materials as reported in the literature [8]. However, there are some issues limiting the usefulness of these materials in SOFC. The electrochemical performance of alkaline earth metal doped lanthanum manganite and ferrites has been reported to decrease with the reduction of temperature due to its low electrical conductivity [9,10]. Another problem arises due to the mismatch of thermal expansion with the electrolytes [11, 12]. The efficiency of $LaMnO_3$ is less at high temperature [13-15]. To conquer this problem, we decided to dope Ba^{2+} at A-site with fixed concentration to create the charge imbalance and hence increased conductivity. The other approach is to compensate the unbalanced charge due to formation of oxygen vacancies by cation substitution of Fe^{3+} at B-site. In the present work, Ba^{2+} and Fe^{3+} co-doped $LaMnO_3$ was synthesized as $(La_{0.7}Ba_{0.3})(Fe_xMn_{1-x})O_3$, where x = 0.1, 0.2, 0.3, 0.4, 0.5 and the samples were characterized for the structural, dielectric and ac-conductivity measurements.

II. EXPERIMENTAL

The $(La_{0.7}Ba_{0.3})(Fe_xMn_{1-x})O_3$, where x = 0.1, 0.2, 0.3, 0.4 and 0.5 ceramic solid solutions were prepared using solid state route. Raw materials La_2O_3, Ba_2CO_3, Fe_2O_3, Mn_2O_3 (from sigma Aldrich, 99.9% pure) were weighted in stoichiometric proportion. The mixed powder was transferred in a bottle containing zirconia balls, propanol (solvent) and mixed using normal ball milling for 24 hours. The mixed dried powder was then exposed to calcination in high temperature furnace at 1200°C for 12 hours. 2 wt % PVA binder was then mixed with calcined powder. Pellets of 10 mm diameter and 1mm thickness were made from the prepared powder with the help of hydraulic press. The pellets were then sintered at 1400°C for 2 hours. The XRD data of the prepared powder was taken from 20° to 80°. FE-SEM measurements were performed to understand the surface morphology.

Manuscript published on 30 September 2019
* Correspondence Author
   Surinder Paul*, I.K.Gujral Punjab Technical University, Kapurthala , Punjab, India
   Manokamna, I.K.Gujral Punjab Technical University, Kapurthala , Punjab, India
   Shubhpreet Kaur, MFM Lab, Department of Physics, Guru Nanak Dev University, Amritsar , Punjab, India
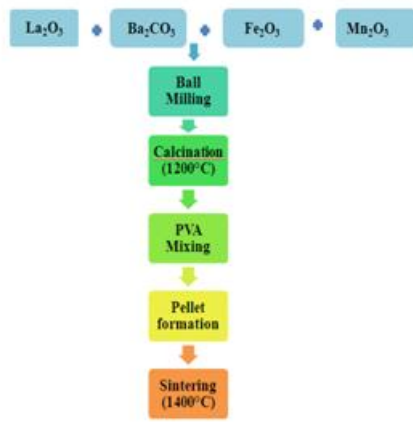   **P.S.Malhi,** Department of Physics, Guru Nanak Dev University, Amritsar , Punjab, India
   Anupinder Singh, Department of Physics, Guru Nanak Dev University, Amritsar , Punjab, India
   Arvind Kumar, Beant College of Engineering & Technology, Gurdaspur, Punjab, India

0.5	5.559	13.565	2.440	419.19

III. RESULTS AND DISCUSSION

A. XRD

XRD patterns of (La$_{0.7}$Ba$_{0.3}$)(Fe$_x$Mn$_{1-x}$)O$_3$ are shown in Figure 1. The high intense peaks show the crystalline nature of the prepared samples. For the structural information (lattice parameters), the Lebail fitting was carried out using hexagonal primitive space group (R-3c, Group no. 167) using FULL PROF SUITE Software.
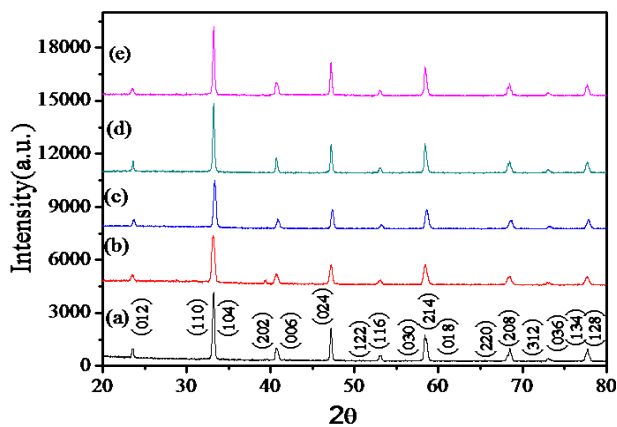

Figure 1: XRD pattern of (La$_{0.7}$Ba$_{0.3}$)(Fe$_x$Mn$_{1-x}$)O$_3$ solid solutions with (a) x = 0.1, (b) x = 0.2, (c) x = 0.3, (d) x = 0.4 and (e) x = 0.5.

The experimental data and theoretical data were quite well matched indicating that the two models are very close to each other. All the peaks are indexed according to R-3c space group and no peak was left unassigned, which indicates that the prepared solid solutions were crystallized into a single phase. The various parameters are tabulated in Table 1.

Table 1: Lattice Parameters of (La$_{0.7}$Ba$_{0.3}$)(Fe$_x$Mn$_{1-x}$)O$_3$with x = 0.1, 0.2, 0.3, 0.4 and 0.5.

Composition (x)	a (Å)	c (Å)	c/a	V (Å^3)
0.1	5.559	13.545	2.436	418.57
0.2	5.559	13.551	2.437	418.75
0.3	5.558	13.557	2.439	418.79
0.4	5.558	13.561	2.439	419.04

B. SEM

The micrographs of (La$_{0.7}$Ba$_{0.3}$)(Fe$_x$Mn$_{1-x}$)O$_3$, where x= 0.1 - 0.5 were collected using Scanning Electron Microscope as shown in Figure 2. It is clear from images that microstructures consist of non-uniform, randomly oriented grains and the average grain size has continuously decreased with increasing substitution of Fe ion at B-site. The density of the samples was examined using Archimedes Principle and the density values were calculated to be 6.7851, 6.6913, 6.6232, 6.2201, 5.5589 for x = 0.1 - 0.5, respectively. The decrease of average grain size shows good agreement with the density of prepared samples.
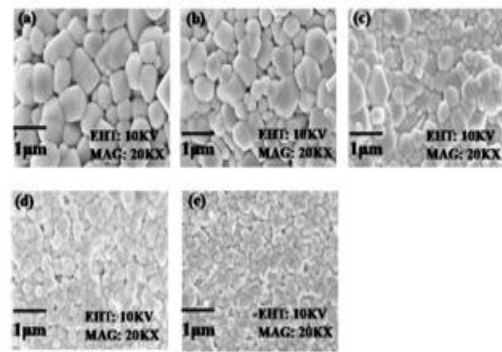

Figure 2: SEM images of La$_{0.7}$Ba$_{0.3}$(Fe$_x$Mn$_{1-x}$)O$_3$ solid solutions with (a) x = 0.1, (b) x = 0.2, (c) x = 0.3, (d) x = 0.4, and (e) x = 0.5.

C. Electrical Conductivity Profile

The electrical conductivity versus temperature profile ranging from room temperature to 600°C at different frequencies of prepared samples of (La$_{0.7}$Ba$_{0.3}$)(Fe$_x$Mn$_{1-x}$)O$_3$, where x= 0.1 and 0.5 is shown in Figure 3. The conductivity for all the samples was calculated using the formula $G\left(\frac{l}{A}\right)= \sigma_{ac}$, where σ_{ac} is the ac conductivity, G is the conductance, l is thickness and A is the area of the electrode. It is clearly seen from the graphs that the conductivity continuously increases with the increase in both temperature and the content of Fe substitution.
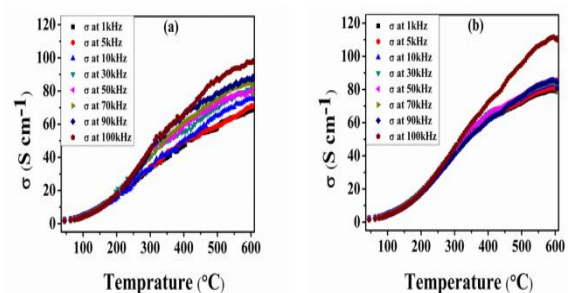

Figure 3: Electrical conductivity as a function of temperature of La$_{0.7}$Ba$_{0.3}$)(Fe$_x$Mn$_{1-x}$)O$_3$ ceramic solid solutions with (a) x = 0.1 and (b) x = 0.5.

The maximum value of the conductivity obtained for the sample with $x = 0.1$ is 98.87 Scm^{-1} and for the sample with $x = 0.5$ is 127 S cm^{-1}, which shows that the Fe substitution in the resulting solid solution increases the conductivity. The activation energy was determined by the Arrhenius fitting of conductivity vs. temperature data as shown in Figure 4. The obtained energy values of $(La_{0.7}Ba_{0.3})(Fe_xMn_{1-x})O_3$ with $x = 0.1$ for the low temperature region (room temperature - 230°C) and for the high temperature region (350°C -600°C) are 0.227eV and 0.1407eV, respectively, whereas for sample with $x = 0.5$, the activation energy reduces to the value of 0.0762eV. The activation energy values are found to be in good agreement with results of the electrical conductivity profile.
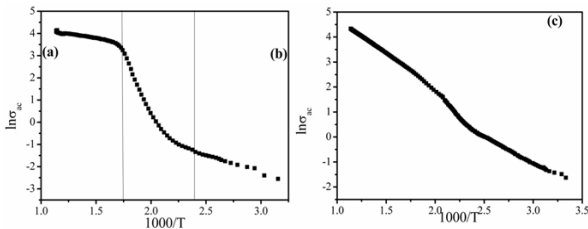

Figure 4: Profile of lnσ vs. 1000/T of $(La_{0.7}Ba_{0.3})(Fe_xMn_{1-x})O_3$, ceramic solid solutions for Fe substitution with $x = 0.1$ for high and low temperature region, shown as (a) & (b), respectively and with $x = 0.5$ as shown in (c).

The electrical conductivity (σ_{ac}) vs. frequency profile at different temperatures is shown in Figure 5. The electrical conductivity is calculated by using a relation $\sigma_{ac} = \omega \varepsilon \varepsilon_0 \tan\delta$, where ε_0 is permittivity in free space and ω is the angular frequency. It is clearly seen from figure 5 that σ_{ac} increases with increase in temperature.

D. Temperature Dependent Dielectric Data

The temperature dependent Dielectric constant ε' and ε'' vs. frequency at different temperature are shown in Figure 6 and 7, respectively. ε' graphs are fitted with Cole-Cole equation [16] representing a relaxation model that is used to describe dielectric relaxations, where the exponent α, is a parameter used to describe different spectral shapes.
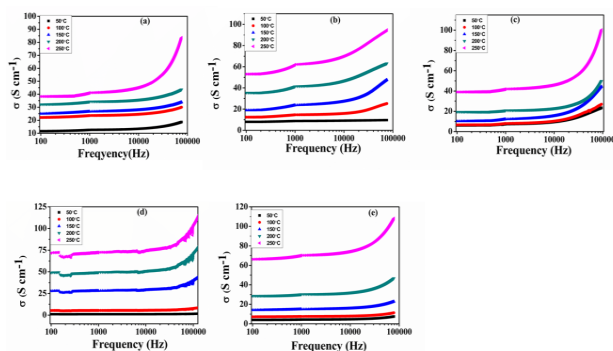

Figure 5: Electrical conductivity response with frequency of $(La_{0.7}Ba_{0.3})(Fe_xMn_{1-x})O_3$, ceramic solid solutions for Fe substitution with (a) x = 0.1, (b) x = 0.2, (c) x = 0.3, (d) x = 0.4 and (e) x = 0.5.

For $\alpha = 0$, the Cole-Cole model reduces to Debye behavior and the relaxation is stretched for α > 0, suggesting that the system moves towards non-Debye behavior. It is clear from the Table 2, that the exponent, α - values are

greater than zero suggesting that the system exhibits non-Debye relaxation.

$$\varepsilon' = \varepsilon_\infty + \frac{(\varepsilon_0 - \varepsilon_\infty)(1 + (\omega\tau)^{(1-\alpha)} \sin\frac{\alpha\pi}{2})}{(1 + 2(\omega\tau)^{(1-\alpha)} \sin\frac{\alpha\pi}{2} + (\omega\tau)^{2(1-\alpha)})}$$

Table 2: The values of α - parameter at different temperature of $(La_{0.7}Ba_{0.3})(Fe_xMn_{1-x})O_3$ solid solutions for Fe substitution with $x = 0.1, 0.2, 0.3, 0.4$ and 0.5.

T (°C)	x = 0.1	x = 0.2	x = 0.3	x = 0.4	x = 0.5
50	0.55722	0.55731	0.55717	0.56875	0.56711
100	0.51249	0.48412	0.50874	0.49573	0.50576
150	0.40480	0.40378	0.40558	0.40452	0.35981
200	0.36759	0.37331	0.36771	0.35878	0.34557
250	0.4102	0.29764	0.29129	0.30765	0.29123

It is clearly revealed from Figure 6 and 7 that both ε' and ε'' continuously decrease with increasing frequency (in lower region) at all temperatures and almost shows a linear behavior in high frequency region. The dipolar relaxation phenomenon [17] very well explains this type of behavior. In lower frequency region, all kinds of the polarization, such as, dipolar, electronic and ionic etc. play an important role and result in the maximum polarizability.
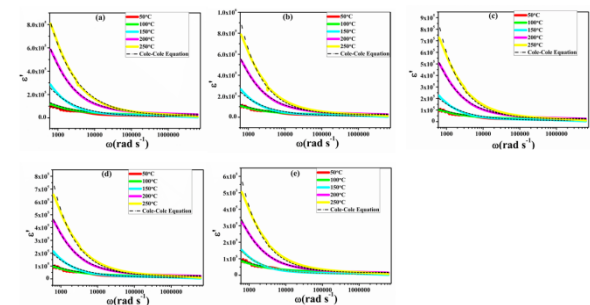

Figure 6: Dielectric constant ε' vs. frequency response of $(La_{0.7}Ba_{0.3})(Fe_xMn_{1-x})O_3$, ceramic solid solution for Fe substitution with (a) $x = 0.1$, (b) $x = 0.2$, (c) $x = 0.3$, (d) $x = 0.4$ and (e) $x = 0.5$.

Figure 7: Dielectric constant ε'' vs. frequency of $(La_{0.7}Ba_{0.3})(Fe_xMn_{1-x})O_3$, ceramic solid solution for Fe substitution with (a) $x = 0.1$, (b) $x = 0.2$, (c) $x = 0.3$, (d) $x = 0.4$ and (e) $x = 0.5$.

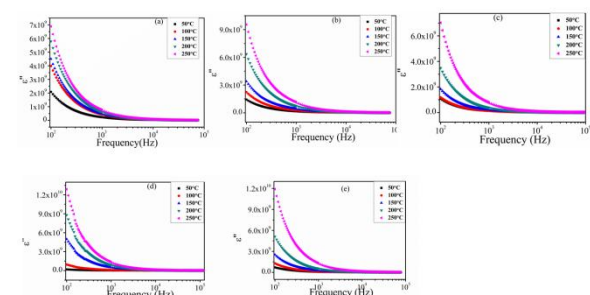# Structural, Dielectric and Electrical Properties of Fe Doped La$_{0.7}$Ba$_{0.3}$MnO$_3$Solid Solutions for Cathode Materials

As the frequency increases, both ε′ and ε″ lag behind the switching signal of dipolar orientation, which results in almost linear variation in higher frequency region due to filtering out of some of the polarizations from the polarizability. Therefore, net polarization of both ε′ and ε″ in higher frequency region becomes less. It has been clearly seen from the graphs that the ε′ and ε″ increases with increasing Fe content. This increase may be due to the contribution of interfacial polarization and not due to the dipolar polarization.

E. Impedance Spectroscopy

The Z′ vs. frequency in temperature range 50°C to 250°C are shown in Figure 8. It is clearly evident that the magnitude of Z′ is high at low temperature and decreases with increase in frequency, which shows a typical negative temperature coefficient of resistance type behavior [18].
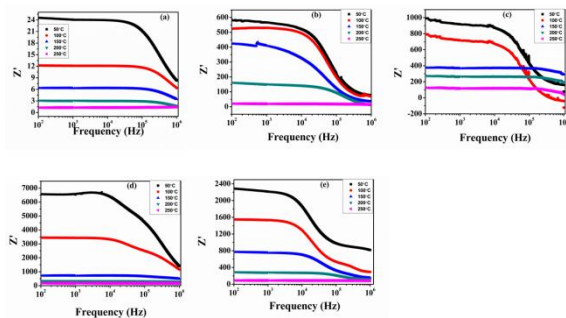

Figure 8: Z' vs. frequency response of (La$_{0.7}$Ba$_{0.3}$)(Fe$_x$Mn$_{1-x}$)O$_3$, ceramic solid solution for Fe substitution with (a) $x = 0.1$, (b) $x = 0.2$, (c) $x = 0.3$, (d) $x = 0.4$ and (e) $x = 0.5$.

The value of Z′ decreases with increase in both temperature and frequency shows the incease in the electrical conductivity [19,20]. Z′ merges in high frequency region at all temperatures showing the reduction of barier properties in the material [21,22].
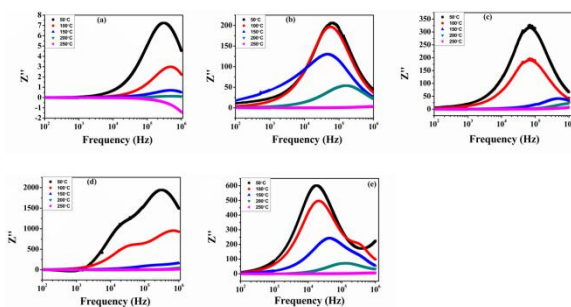

Figure 9: Z'' vs. frequency of (La$_{0.7}$Ba$_{0.3}$)(Fe$_x$Mn$_{1-x}$)O$_3$, ceramic solid solution for Fe substitution with (a) $x = 0.1$, (b) $x = 0.2$, (c) $x = 0.3$, (d) $x = 0.4$ and (e) $x = 0.5$.

The behaviour of imaginary part of impedance, Z″ as a function of frequency at different temperatures is shown in Figure 9. The decreasing nature of Z″ with increase in both temperature and frequency reveals the reduction of the resistive properties of the material. The broading of peaks with increase in temperature confirms the temperature dependent electrical relaxation phenomenon in the prepared samples. In high frequency region, Z″ curves merge revelaing the disappearnce of space charge polarization [23,24].

IV CONCLUSIONS

(La$_{0.7}$Ba$_{0.3}$)(Fe$_x$Mn$_{1-x}$)O$_3$, where $x = 0.1 - 0.5$ perovskite solid solutions were synthesized by solid state

reaction route. The XRD analysis confirmed the hexagonal phase structure of all the samples. The micrographs showed that the average grain size continuously decreases with increasing Fe-content which in good agreement with density of prepared samples. The electrical conductivity values at different temperatures and frequencies were found to in increasing order with an increase in doping or Fe substitution. The impedance spectroscopy confirmed the non-Debye relaxation behavior of all the samples.

REFERANCES

1. C. Sun, R. Hui, J. Roller, J Solid State Electrochem (2010) 14:1125-1144.
2. C. W. Sun, U. Stimming, J Power Sources (2007) 171:247.
3. S. C. Singhal, K. Kendall, High temperature solid oxide fuel cells: fundamentals, design, and applications. Elsevier, Oxford, pp 1-22.
4. M. Mogensen, K. Kammer, Annu Rev Mater Res (2003) 33:321.
5. S. J. Skinner, International Journal of Inorganic Materials3 (2001) 113-121.
6. A. J. Casonova, Power Sources, 1998: 71:65.
7. K. Kordesch, G. Simader, Fuel Cells and their Applications, Weinheim, Cambridge, VCH, 1996.
8. P. Plonczak, M. Gazda, B. Kusz, P. Jasinski, Journal of Power Sources 181 (2008) 1-7.
9. H.H. Mobius, J. Solid State Electrochem. **Vol** 1, Pp 2–16 (1997).
10. S. Carter, A. Selcuk, R.J. Chater, J. Kajda, J.A. Kilner, B.C.H. Steele, Solid State Ion.**Vol**53–56, Pp 597–605, (1992).
11. R.A. De Souza, J.A. Kilner, J.F. Walker, Mater. Lett. **Vol** 43, Pp 43–52 (2000).
12. V.V. Srdic, R.P. Omorjan, J. Seydel, Mater. Sci. Eng. B, **Vol** 116, Pp 119–124 (2005)
13. E. Hernandez, V. sagredo and G. E. Delgado, Revista Mexicana de Fisica 61 (2015) 166-169.
14. F. C. C. Moura, M. H. Araujo, J. D. Ardisson, W. A. A. Macedo, A. S. Albuquerque and R.M. Lago, J. Braz. Chem. Soc., Vol. 18, No. 2, 322-329, 2007.
15. F. Bidrawn, S. Lee, J. M. Vohs and R. J. Gorte, Journal of The Electrochemical Society, 155(7) B660-B665 (2008).
16. Cole K.S. Robert H. (1941). Journal of Chemical Physics 9:341-351.
17. M. Kumar, K. L. Yadav, J. Phys.: Condens Matter (2002) 19:242202.
18. T. Badapanda, S. Sarangi, B. Behera, S. Anwar, Structural and impedance spectroscopy study of Samarium modified Barium Zirconium Titanate ceramic prepared by mechanochemical route, Current Applied Physics. 14(2014)1192–1200. doi:10.1016/j.cap.2014.06.007.
19. U. Dash, S. Sahoo, P. Chaudhuri, S.K.S. Parashar, K. Parashar, Electrical properties of bulk and nano Li2TiO3 ceramics: A comparative study, Journal of Advanced Ceramics. 3 (2014) 89–97. doi:10.1007/s40145-014-0094-0.
20. B. Tiwari, R.N.P. Choudhary, Study of Impedance Parameters of Cerium Modified Lead ZirconateTitanate Ceramics, IEEE Transactions on Dielectrics and Electrical Insulation. 17 (2010) 5–17. doi:10.1109/TDEI.2010.5411996.
21. B. Tiwari, R.N.P. Choudhary, Frequency-temperature response of Pb(Zr0.65-xCexTi0.35)O3 ferroelectric ceramics: Impedance spectroscopic studies, Journal of Alloys and Compounds. 493 (2010) 1–10. doi:10.1016/j.jallcom.2009.11.120.
22. H. Singh, A. Kumar, K.L. Yadav, Structural, dielectric, magnetic, magnetodielectric and impedance spectroscopic studies of multiferroic BiFeO3 – BaTiO3 ceramics, Materials Science & Engineering B. 176 (2011) 540–547. doi:10.1016/j.mseb.2011.01.010.
23. R. Ranjan, R. Kumar, B. Behera, R.N.P. Choudhary, Structural and impedance spectroscopic studies of samarium modified lead zirconatetitanate ceramics, Physica B. 404 (2009) 3709–3716.

doi:10.1016/j.physb.2009.06.113

24. M.R. Biswal, J. Nanda, N.C. Mishra, S. Anwar, A. Mishra, Dielectric and impedance spectroscopic studies of multiferroic BiFe1-xNixO3, Advanced Materials Letters. 5(2014) 531–537. doi:10.5185/amlett.2014.4566.

AUTHORS PROFILE

Surinder Paul, research scholar in the field of Applied Physics at I.K.Gujral Punjab Technical University, Kapurthala , Punjab, India

Manokamna,research scholar in the field of Applied hemistry at I.K.Gujral Punjab Technical University, Kapurthala , Punjab, India

Shubhpreet Kaur, MFM Lab, department of Physics, Guru Nanak Dev University, Amritsar, Punjab, India

Er.P.S.Malhi, Department of Chemistry, Guru Nanak Dev University, Amritsar , Punjab, India

Dr. Anupinder Singh, MFM Lab, **D**epartment of Physics, Guru Nanak Dev University, Amritsar, Punjab, India. Studied at IIT Delhi

Dr. Arvind Sharma, Associate professor in Beant College of Engineering & Technology, Gurdaspur, Punjab, India